

Exploring Disentangled and Controllable Human Image Synthesis: From End-to-End to Stage-by-Stage

Zhengwentai Sun^{1,2} Heyuan Li² Xihe Yang² Keru Zheng² Shuliang Ning^{1,2}
Yihao Zhi¹ Hongjie Liao² Chenghong Li^{1,2} Shuguang Cui^{2,1} Xiaoguang Han^{2,1*}

¹FNii, CUHKSZ ²SSE, CUHKSZ



Figure 1. We propose a new task focused on explicit disentanglement of key human attributes within a unified framework, enabling fine-grained controllability in human synthesis. Moreover, we explore to train an end-to-end model and further design a stage-by-stage pipeline for generating human images with customizable inputs, offering enhanced flexibility and superior control over the synthesis process.

Abstract

Achieving fine-grained controllability in human image synthesis is a long-standing challenge in computer vision. Existing methods primarily focus on either facial synthesis or near-frontal body generation, with limited ability to simultaneously control key factors such as viewpoint, pose, clothing, and identity in a disentangled manner. In this paper, we introduce a new disentangled and controllable hu-

man synthesis task, which explicitly separates and manipulates these four factors within a unified framework. We first develop an end-to-end generative model trained on MVHumanNet for factor disentanglement. However, the domain gap between MVHumanNet and in-the-wild data produce unsatisfactory results, motivating the exploration of virtual try-on (VTON) dataset as a potential solution. Through experiments, we observe that simply incorporating the VTON dataset as additional data to train the end-to-end model degrades performance, primarily due to the

*Corresponding author: hanxiaoguang@cuhk.edu.cn

inconsistency in data forms between the two datasets, which disrupts the disentanglement process. To better leverage both datasets, we propose a stage-by-stage framework that decomposes human image generation into three sequential steps: clothed A-pose generation, back-view synthesis, and pose and view control. This structured pipeline enables better dataset utilization at different stages, significantly improving controllability and generalization, especially for in-the-wild scenarios. Extensive experiments demonstrate that our stage-by-stage approach outperforms end-to-end models in both visual fidelity and disentanglement quality, offering a scalable solution for real-world tasks. Additional demos are available on the project page: <https://taited.github.io/discoshuman-project/>.

1. Introduction

Synthesizing human-centric images is crucial for various applications like virtual reality, the metaverse, video games, and digital fashion. Advances in GANs [4, 13, 21] and large-scale facial datasets [20, 29] have enabled realistic face generation [19], with subsequent research focusing on controlling facial appearances and expressions [7, 30, 43], though often limited to frontal views. The introduction of 3D-aware GANs, EG3D [5], brought view controllability, paving the way for unified control over viewpoint, expression, and appearance [1, 2, 26, 27, 38]. Compared with human faces, full-body image generation is more complex due to clothing variations and pose deformations.

Early GAN-based full-body image generation methods [11, 12, 35] supporting pose or appearance editing but restricted to near-frontal views. Following the key idea of EG3D [5], EVA3D [16] also tried to further enable view controllability of human image generation. There are also a specific topic in this area which focus on clothing image synthesis, i.e., virtual try-on [6, 8, 25, 32, 45]. To achieve free-view human image synthesis, disentanglement and controllability have been key research focuses. However, a unified framework addressing all requirements remains challenging, primarily due to the lack of datasets with disentangled factors. The recent release of the multi-view human video dataset, MVHumanNet [40], provides the possibility to take a step forward in this research direction.

To achieve fine-grained controllability over human synthesis, we propose a task that emphasizes explicit disentanglement of facial identity, clothing, pose, and viewpoint within a unified framework. A natural approach to solving this problem is to train an end-to-end model that synthesizes human images while explicitly conditioning on these factors. We attempted to conduct experiments on MVHumanNet to train an end-to-end model. While the model demonstrates a degree of controllability, its robustness and generalizability remain limited when trained exclusively on

this dataset. These limitations primarily stem from inherent issues within the dataset itself. Specifically, MVHumanNet is collected in an indoor environment, which introduces a domain gap when compared to in-the-wild data.

Given these challenges, we explore to incorporate VTON dataset, which contains high-quality clothing images with more detailed textures, combined with MVHumanNet to train end-to-end model. However, our experiments reveal that simply incorporating VTON dataset as additional data to train end-to-end model result in performance degradation rather than improvement. We attribute this decline to the inconsistency in data forms between the two datasets when training the end-to-end model with multiple conditioning factors. Instead of relying on a single end-to-end model, we explore to decompose the synthesis process into sequential stages, with each step focusing on a specific sub-task. This approach offers two advantages: **1)** it enables better dataset utilization by allowing different datasets to specialize in sub-tasks, **2)** improves factor separation by explicitly handling each attribute at distinct stages.

Building on this framework, we designed a three-stage pipeline for generating human images with arbitrary facial identity, clothing, pose and view as input (See Fig. 1). The first stage generates a clothed A-pose human with a specified face and shoes, trained on the VTON dataset. Next, the second stage synthesizes the back view of the human using the MVHumanNet dataset. Finally, the third stage enables the generation of a human image in an arbitrary pose and viewpoint by combining the VTON and MVHumanNet datasets. To condition human synthesis on pose and viewpoint control, we use the 3D parametric model SMPLX [33], and render the SMPLX mesh from a given viewpoint and apply a UV-based texture encoding, where each body part is assigned a unique color-coded coordinate. With these structured controls, we implement a diffusion transformer (DiT)-based [34] architecture for back-view and free-view human synthesis, which integrates these disentangled factors into the synthesis pipeline. By incorporating these structured controls, our approach enables fine-grained manipulation of multiple human attributes within a unified framework. Our experiments demonstrate that, even when using a network structure similar to the end-to-end model, the stage-by-stage approach exhibits significantly better generalizability. This suggests that a stage-by-stage framework can more effectively utilize available data by assigning different datasets to specialized sub-tasks. We also observe that as the conditioning in the third stage becomes simpler, training by combining the MVHumanNet and VTON datasets leads to improved performance compared to training solely on the MVHumanNet dataset.

The contribution can be summarized as follows:

- We introduce a new and challenging task in human image synthesis that aims to achieve explicit disentanglement

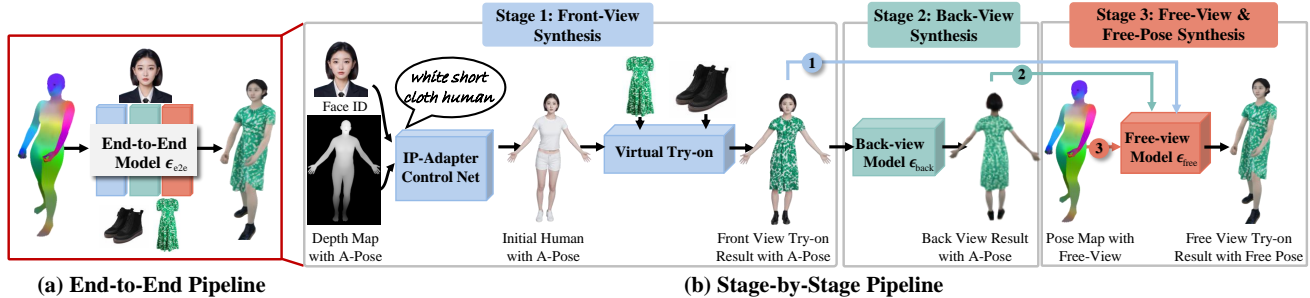


Figure 2. Overview of the proposed pipelines. (a) The end-to-end pipeline directly synthesizes the final image from disentangled inputs, including a face image, clothing images, and a pose map. (b) The stage-by-stage pipeline decomposes the process into three steps: front-view synthesis with identity and clothing control, back-view synthesis, and free-view synthesis under the target pose and viewpoint. Both pipelines are implemented using DiscoHuman, with details provided in Fig. 3.

and control over viewpoint, pose, clothing, and identity within a unified framework.

- We explore a novel end-to-end model that can address the disentangled and controllable human synthesis task and further propose a stage-by-stage framework that enhances control over pose and viewpoint, significantly improving generalizability, particularly for in-the-wild scenarios.
- Our experiments demonstrate that our methods achieve effective disentanglement, outperforming existing methods in view and pose control. We hope that our experiments and discussion on end-to-end versus stage-by-stage methods will inspire relevant human synthesis research.

2. Related Work

2.1. Human Synthesis

In the realm of human synthesis, recent works [9, 11, 12, 16, 17, 35, 39, 46, 49] have advanced the field by focusing on generating high-quality, full-body human images with diverse identities, hairstyles, garments, and poses. StyleGAN-Human [12] adopts a data-centric perspective to examine the data factors influencing image generation based on the StyleGAN framework. InsetGAN [11] integrates multiple pre-trained GANs, with each focusing on distinct components. To achieve control over pose, local body part appearance and garment style, HumanGAN [35] is capable of performing all tasks related to global appearance sampling, pose transfer, part and garment transfer, as well as part sampling. EVA3D [16] and Get3DHuman [39] expand the synthesis capabilities beyond 2D, pushing toward 3D human generation with realistic texture and pose control. EVA3D [16] incorporates a compositional human NeRF (Neural Radiance Field) representation, which divides the human body into 16 distinct parts and assigns each part an individual network. Each network models the corresponding local volume, allowing EVA3D to capture detailed textures and pose variations with high accuracy. Get3DHuman [39], lifting StyleGAN-Human into 3D, advances full-body human syn-

thesis and enables detailed control over body shape, garment, and even facial expression, making it highly applicable in applications like gaming, virtual reality, and digital fashion.

2.2. Pose Transfer

With the growing prominence of diffusion models, increasing research attention [3, 14, 18, 31, 37, 42] has shifted toward realistic person image generation using the powerful frameworks. PIDM [3] pioneers the utilization of denoising diffusion models for person image synthesis, showcasing their ability to produce high-quality images through iterative noise removal. Expanding on this, PoCoLD [14] incorporates pose constraints into a latent diffusion model, enabling more flexible and controlled image synthesis in the latent space by modulating the subject’s pose. PCDMs [37] introduces a progressive conditional diffusion framework that refines pose-guided image synthesis step-by-step to enhance pose control. CFLD [31] employs a coarse-to-fine latent diffusion framework to enhance control over pose manipulation and improve the realism of synthesized images by progressively refining details from coarse to fine levels in the latent space. MagicAnimate [42] and Animate Anyone [18] further extend diffusion models’ capabilities by focusing on animating person images, enabling smooth transitions between different poses and movements to produce high-quality dynamic effects for virtual characters. Human4DiT [36] proposes a novel framework for generating 360-degree high-quality, spatio-temporally coherent human videos from a single image, combining diffusion transformers for global correlation modeling to achieve fine-grained control over pose and viewpoint.

2.3. Virtual Try-on

Image-based virtual try-on (VTON) synthesizes realistic images by transferring garment appearances onto their bodies. Recent methods use GANs or diffusion models to improve realism and precision. GAN-based approaches like

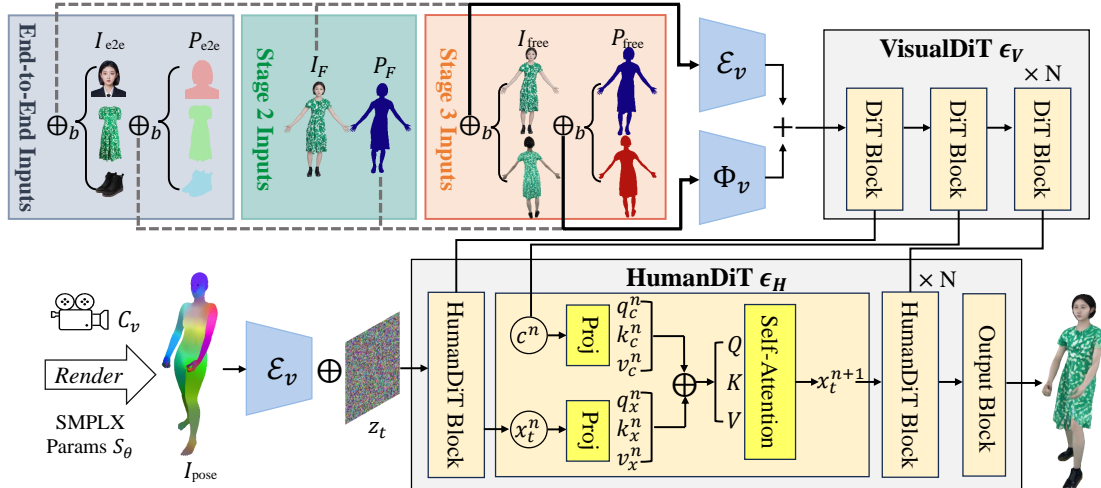


Figure 3. DiscoHuman model ϵ consists of a VisualDiT ϵ_V and a HumanDiT ϵ_H . The VisualDiT is responsible for encoding visual conditions, with different input settings depending on the pipeline or stage in which DiscoHuman is applied. The upper left blocks illustrate three possible input configurations. In this figure, the active configuration corresponds to Stage 3, while the inactive settings are indicated by grey dashed lines. To maintain simplicity, the denoising timestep t is not shown in this figure.

VITON-HD [6] address high-resolution image misalignment with ALIAS normalization, while HR-VITON [25] integrates warping and segmentation into a unified try-on condition generator to reduce artifacts. However, GAN-based models often produce unnatural deformations in wild scenarios, reducing the fidelity and realism of the output result. In contrast, diffusion models have recently demonstrated strong performance in image generation. OOTDiffusion [41] aligns garment features with bodies using Outfitting Fusion, improving realism and controllability without redundant warping. IDM-VTON [8] employs a visual encoder and parallel UNet for better garment encoding, while DressCode [32] introduces a multi-category dataset and a Pixel-level Semantic-Aware Discriminator (PSAD) to enhance image quality and realism. CAT-DM [45] leverages ControlNet to add control conditions and enhance garment feature extraction.

3. Method

3.1. Overview

Fig. 2 provides an overview of the proposed pipelines for human image synthesis: an end-to-end pipeline and a stage-by-stage pipeline. Both pipelines leverage the proposed DiT-based model, **DiscoHuman**, which enables **disentangled** and **controllable human** synthesis.

The end-to-end pipeline directly generates a complete human image from a set of disentangled inputs, including a face image, clothing images (upper/lower clothing or a dress, and shoes), and a pose map, allowing simultaneous control over face identity, clothing, pose, and viewpoint. In contrast, the stage-by-stage pipeline refines the synthesis

process in three stages. It first generates an A-pose human image with identity and clothing control, then estimates the back view, and finally synthesizes a free-view image under a target pose and viewpoint. This decomposition enhances controllability and generalizability. DiscoHuman is adapted for the second and third stage by modifying its input configurations. Architectural details of DiscoHuman are further described in Sec. 3.2.

3.2. DiscoHuman

We developed DiscoHuman for disentangled and controllable human synthesis. Fig. 3 illustrates its structure. Given a set of disentangled conditions, it enables fine-grained control over appearance, pose, and viewpoint in human image generation. The model consists of two key components: VisualDiT Encoder, which encodes appearance-related conditions, and HumanDiT, which synthesizes the final human image while ensuring spatial alignment with the input pose.

VisualDiT Encoder The VisualDiT Encoder is a DiT-based module specifically designed for encoding visual conditions. Unlike standard DiT models, which take a noised latent as input, VisualDiT processes un-noised latents extracted from input images and conditions the denoising timestep at a fixed value t_0 .

A major challenge in implementing VisualDiT is the variation in both the quantity and semantics of input conditions. For instance, a sample may include two clothing images (upper and lower garments) or just one image (a full-body dress). A naive solution would involve designing separate encoders for different semantic categories, but this leads to unacceptable computational overhead.

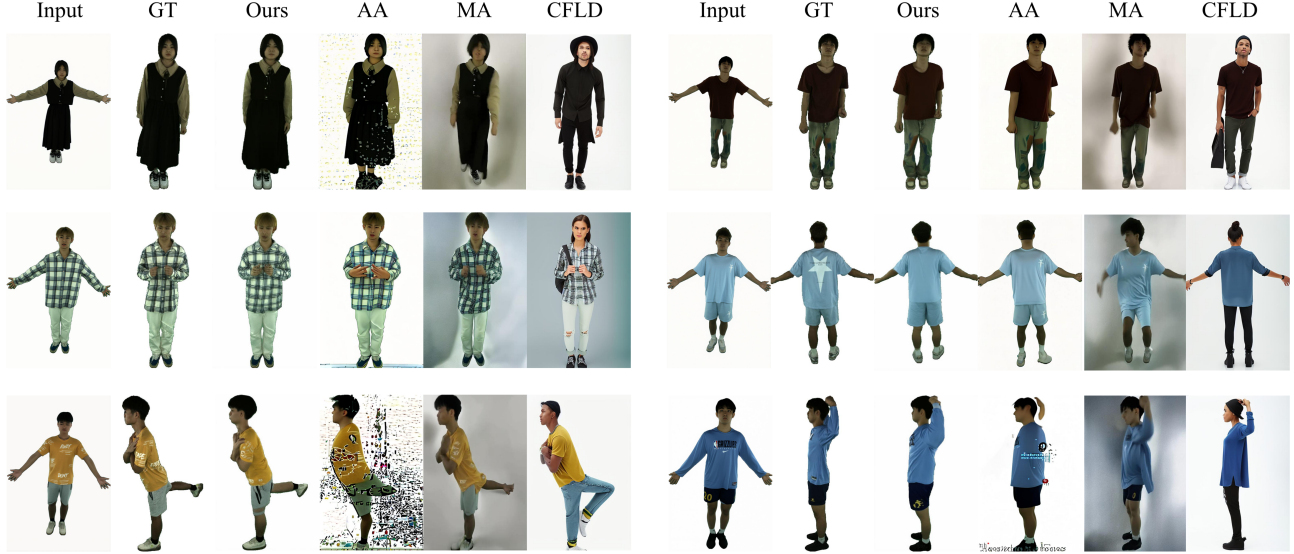


Figure 4. Qualitative comparison of different methods on MVHumanNet [40] datasets. Note that AA stands for AnimateAnyone and MA stands for MagicAnimate.

To address this, the VisualDiT Encoder adopts a unified processing strategy. Given a set of image conditions $I = \{I_1, I_2, \dots, I_n\}$, each image is first passed through a VAE encoder $\mathcal{E}_v(\cdot)$ to obtain its latent representation. Meanwhile, the corresponding foreground segmentation masks $P = \{P_1, P_2, \dots, P_n\}$ are one-hot encoded to indicate their semantic categories. A semantic embedding function $\Phi_v(\cdot)$, implemented as a convolutional layer, is applied to these segmentation maps to ensure compatibility with the image latents.

The VisualDiT Encoder then processes the concatenated image latents and embedded semantic maps, producing multi-level condition features c^n at each DiT block:

$$c^n = \epsilon_V (\mathcal{E}_v(\oplus_b I) + \Phi_v(\oplus_b P), t_0), \quad (1)$$

where the superscript n indicates the index of the DiT block, ϵ_V denotes VisualDiT, $\mathcal{E}_v(\cdot)$ is the VAE encoder, and \oplus_b represents batch-wise concatenation.

HumanDiT The HumanDiT model synthesizes the final human image based on the multi-level condition features c^n and a viewpoint-conditioned pose representation. To achieve precise pose and viewpoint control, we utilize the 3D parametric model SMPLX [33]. The SMPLX mesh is rendered under the target viewpoint, providing a structured pose representation that encodes both articulation and spatial alignment. The resulting pose map I_{pose} is then processed through the VAE encoder $\mathcal{E}_v(\cdot)$ to ensure consistency with the visual condition features.

The HumanDiT model conditions the synthesis process on these features, formulated as:

$$\hat{\epsilon}_t = \epsilon_H (z_t \oplus \mathcal{E}_v(I_{\text{pose}}), t, c^n), \quad (2)$$

where ϵ_H represents the HumanDiT model, z_t is a random noise latent, and \oplus denotes channel-wise concatenation. The pose map I_{pose} is processed using the VAE encoder $\mathcal{E}_v(\cdot)$, aligning its representation with the image features.

Within each DiT block of ϵ_H , effective feature fusion is essential. To achieve this, the diffusion feature x_t^n and the multi-level condition features c^n are separately projected into query (q), key (k), and value (v) representations, which are concatenated in a length-wise manner:

$$\mathbf{Q} = q_x^n \oplus q_c^n, \quad \mathbf{K} = k_x^n \oplus k_c^n, \quad \mathbf{V} = v_x^n \oplus v_c^n. \quad (3)$$

A self-attention mechanism is then applied to fuse these features, allowing the HumanDiT model to effectively reference the conditioning information:

$$\hat{x}_t^{n+1} = \text{softmax} \left(\frac{\mathbf{Q}\mathbf{K}^T}{\sqrt{d}} \right) \mathbf{V}. \quad (4)$$

Since concatenating c^n increases the sequence length, the excess portion is discarded after attention to maintain computational efficiency.

Rectified Flow Loss To optimize the entire DiscoHuman model ϵ , we applied rectified flow [10, 28]. The forward and corresponding loss function are defined as follows:

$$\hat{\epsilon}_t = \epsilon (z_t, I_{\text{pose}}, t, I, P), \quad (5a)$$

$$\mathcal{L} = \mathbb{E}_{t, x_0, x_t} \left[w(t) \| \hat{\epsilon}_t - (x_t - x_0) \|^2 \right], \quad (5b)$$



Figure 5. Qualitative comparison of different methods on sampled results from THuman4.0 [50] (bottom) and AvatarRex [51] (top) datasets. Note that AA stands for AnimateAnyone and MA stands for MagicAnimate.

where $w(t)$ is a weighting function [10], x_0 is the latent representation of the ground truth image, and x_t represents noised x_0 at timestep t .

3.3. End-to-End (E2E) Pipeline

In the end-to-end pipeline, we extract controllable factors from an A-pose image using SMPLX parameters and segmented face and clothing images. The inputs image and corresponding parsing maps to the VisualDiT Encoder are defined as:

$$I_{e2e} = \{I_{\text{face}}, I_{\text{upper cloth}}, I_{\text{lower cloth}}, I_{\text{dress}}, I_{\text{shoes}}\}, \quad (6a)$$

$$P_{e2e} = \{P_{\text{face}}, P_{\text{upper cloth}}, P_{\text{lower cloth}}, P_{\text{dress}}, P_{\text{shoes}}\}. \quad (6b)$$

The input settings for HumanDiT remain consistent with those described in Sec. 3.2. Since a person’s outfit consists of either separate garments (upper and lower) or a whole-body dress, we ensure consistency by inputting a black image with a semantic map labeled as pure ‘background’ whenever a clothing category is missing. To train the e2e model, the forward process is defined as follows:

$$\hat{\epsilon}_t = \epsilon_{e2e}(z_t \oplus \mathcal{E}_v(I_{\text{pose}}), t, I_{e2e}, P_{e2e}), \quad (7)$$

where ϵ_{e2e} is the DiscoHuman model applied in end-to-end pipeline.

3.4. Stage-by-Stage (SBS) Pipeline

Stage 1: Front-View Synthesis The first stage provides initial control over face identity and clothing. This process consists of two steps. First, IP-Adapter [44] is used to control face identity, while ControlNet [48] ensures that the human pose is fixed in an A-pose. A simple text prompt is used to generate a person wearing a tight white T-shirt and trousers, which simplifies the subsequent try-on process. Next, given the target clothing, IDM-VTON [8] is applied to generate the try-on results. Since no dedicated model exists for shoe try-on, IP-Adapter with image-guided inpainting is used to apply shoes to the synthesized person.

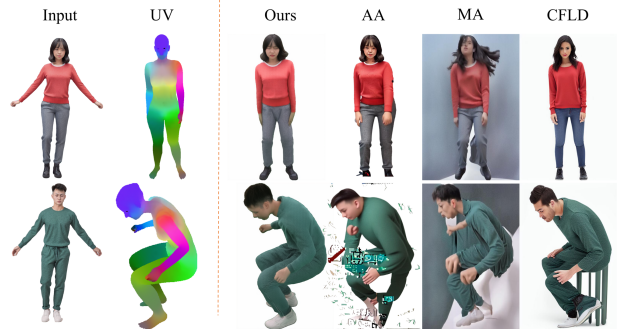


Figure 6. Qualitative zero-shot inference results of different methods on in-the-wild full-body human images generated by Stable Diffusion.

Stage 2: Back-View Synthesis The second stage synthesizes a realistic back-view image I_B of the previous generated front-view image I_F . This is achieved by reusing the DiscoHuman model with modified inputs in the VisualDiT Encoder, where the front-view image serves as the visual condition. Since only the front image is available, the corresponding semantic map is derived from its foreground segmentation as P_F . The back-view generation model is formulated as follows:

$$\hat{\epsilon}_t = \epsilon_{\text{back}}(z_t, I_{\text{A-pose}}, t, I_F, P_F). \quad (8)$$

During training, we observe significant lighting shifts between the front and back camera views in the MVHumanNet dataset. Directly using raw MVHumanNet images introduces color saturation shifts, leading to unrealistic textures in the synthesized back views. To mitigate this issue, we employ the FLUX [24] model to enhance the training image quality, particularly in frontal and back A-pose images. As demonstrated in our ablation study in Sec. 4.3, this enhancement significantly improves synthesis quality.

Stage 3: Free-View & Pose Synthesis The final stage generates a human image under an arbitrary pose and viewpoint using the outputs from Stage 1 and Stage 2 along with a pose map. To obtain the foreground segmentation map of I_F and I_B , SAM model [23] is applied to obtain P_F and P_B . Thus we have $I_{\text{free}} = \{I_F, I_B\}$, $P_{\text{free}} = \{P_F, P_B\}$. The free-view synthesis model is formulated as follows:

$$\hat{\epsilon}_t = \epsilon_{\text{free}}(z_t, I_{\text{pose}}, t, I_{\text{free}}, P_{\text{free}}). \quad (9)$$

4. Experiments

4.1. Implementation Details

In the implementation of DiscoHuman, both VisualDiT and HumanDiT utilize the pre-trained DiT model from Stable Diffusion 3 Medium [10], which consists of 24 DiT blocks. To conserve GPU memory, VisualDiT employs only the first 12 blocks. The corresponding block features c^n from

Dataset	MVHumanNet [40]				THuman 4.0 [50]				AvatarReX [51]			
	Method	FID ↓	LPIPS ↓	PSNR ↑	SSIM ↑	FID ↓	LPIPS ↓	PSNR ↑	SSIM ↑	FID ↓	LPIPS ↓	PSNR ↑
AnimateAnyone [18]	70.7821	0.4331	13.2582	0.6750	74.1451	0.2642	14.7458	0.7799	69.2732	0.2157	15.5053	0.8264
MagicAnimate [42]	63.4553	0.4798	9.3189	0.7180	96.6649	0.4844	8.3149	0.6974	102.0733	0.5225	7.4551	0.6911
CFLD [31]	56.4594	0.2624	13.4898	0.7878	80.4250	0.2626	13.7125	0.7765	78.8488	0.2281	14.6376	0.8179
Ours (SBS)	14.4210	0.1622	17.0370	0.8311	58.5134	0.2262	14.7664	0.7870	53.0746	0.1744	16.1607	0.8378

Table 1. Quantitative evaluation on MVHumanNet [40], THuman 4.0 [50], and AvatarReX dataset [51]. The comparison on THuman 4.0 and AvatarReX is conducted in a zero-shot manner. Cells highlighted in denotes the best and second-best performances.

VisualDiT are duplicated across all blocks to ensure alignment with HumanDiT. The synthesis resolution for the image is set to 512×768 . For hyperparameter settings, we use an 8-bit Adam optimizer with a learning rate of 2×10^{-5} and a batch size of 16. All experiments are conducted on two A100 GPUs for 30k training steps. Due to the page limitation, in terms of the dataset preparation, please refer to the supplementary material.

Method	FLUX	FID ↓	LPIPS ↓	PSNR ↑	SSIM ↑
Back-View Model	✓	38.5276	0.1852	15.3949	0.8077
Back-View Model		46.0028	0.1723	15.6032	0.8179
Free-View Model	✓	20.8115	0.1711	16.9394	0.8275
Free-View Model		27.2246	0.1790	15.9477	0.8090

Table 2. Ablation study on FLUX enhancement for back-view model training of the stage-by-stage pipeline. We mark the best results with .

Method	Training Dataset	FID ↓	LPIPS ↓	PSNR ↑	SSIM ↑
E2E	MVHumanNet + VTON	25.1648	0.4494	10.7573	0.6606
E2E	MVHumanNet	20.7037	0.3747	12.5632	0.7294
SBS	MVHumanNet + VTON	14.4210	0.1622	17.0370	0.8311
SBS	MVHumanNet	20.8115	0.1711	16.9394	0.8275

Table 3. Quantitative results of end-to-end (E2E) vs. stage-by-stage (SBS) training under different dataset combinations. We mark the best and second-best results with .

4.2. Comparison

In this section, we primarily present the results of the Stage-by-Stage pipeline, as it achieves the best performance. Since Stage 1 (Front-View Synthesis) relies on pre-trained models, we focus our comparison on Stage 2 and Stage 3 to fairly evaluate our contributions. These two stages together can be interpreted as a pose transfer framework, making them directly comparable to SOTA pose transfer methods.

We therefore compare our approach with AnimateAnyone [18], MagicAnimate [42], and CFLD [31]. Since the official implementation of AnimateAnyone has not been released, we use a third-party reimplementation*.

*Moore-AnimateAnyone: <https://github.com/MooreThreads/Moore-AnimateAnyone>

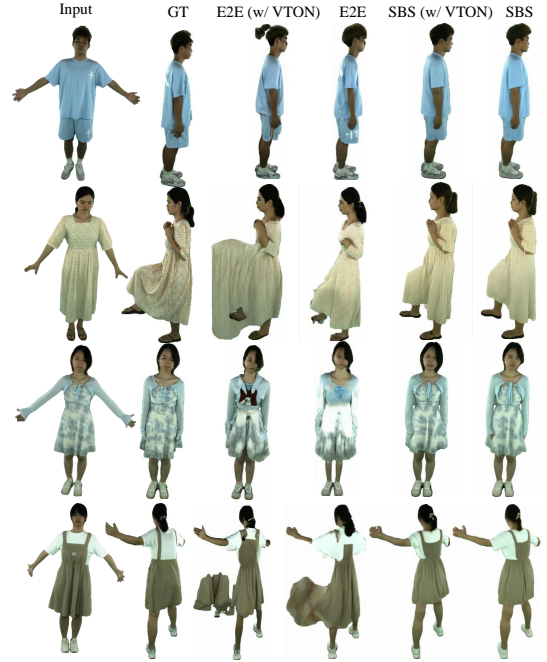


Figure 7. Qualitative comparison for End-to-End (E2E) and Stage-by-Stage (SBS) results on MVHumanNet [40] dataset.

Qualitative Evaluation Fig. 4 presents the qualitative results on the MVHumanNet dataset. Our method achieves the best performance across various views and poses. For instance, the first example in the third row of Fig. 4 demonstrates a challenging view and pose transfer. Our model accurately generates the corresponding pose for the given view, whereas other methods fail to synthesize a plausible right leg of the input identity.

In addition to the evaluation on MVHumanNet, we also demonstrate our method’s zero-shot capability on the THuman 4.0 [50] and AvatarReX [51] datasets shown in Fig. 5, since none of the comparison methods were trained on these datasets. Nevertheless, our method performs well, while AnimateAnyone and MagicAnimate exhibit lower pose accuracy. As for CFLD, it fails to faithfully preserve the identity of the input reference human. We also apply our Stage-by-Stage framework to in-the-wild human images. From Fig. 6, our method performs well for pose and view control

with consistent identity, while other methods fail to faithfully preserve the factors of the input reference human.

Quantitative Evaluation Tab. 1 presents the quantitative evaluation results of our method. To assess the quality of the synthesized images, we use FID, LPIPS, PSNR, and SSIM as evaluation metrics. Our method achieves the best overall performance across all datasets and metrics.

Notably, the results on THuman 4.0 and AvatarReX are evaluated in a zero-shot setting, further demonstrating the robustness and generalizability of our stage-by-stage (SBS) pipeline. On THuman 4.0 dataset, AnimateAnyone achieves comparable performance in LPIPS, PSNR, and SSIM; however, its FID score is significantly worse than ours, indicating lower perceptual quality. The results show that our method performs consistently well and remains robust across varying numbers of views when generating free-view images. Additionally, CFLD achieves the second-best performance on MVHumanNet, suggesting that it is well-suited for scenarios with fewer viewpoints. However, as the number of views increases, AnimateAnyone outperforms CFLD and becomes the second-best model. Our method, in contrast, remains robust across different view settings, demonstrating its superior adaptability to view variations.

4.3. Ablation Study

During Stage 2 Back-View Synthesis, we find that directly using a front-view A-pose image to predict its back-view counterpart is highly challenging. This difficulty arises not only from the missing information on the back but also from the inconsistent lighting conditions in the MVHumanNet dataset. As a result, if we explicitly use the synthesized back-view results in Stage 3, we observe notable degradation in performance compared to the training setup, which uses a ground-truth A-pose back-view image as input.

To address this, we conduct an ablation study and find that enhancing the quality of front-back A-pose images significantly improves the performance of both the back-view synthesis model and the free-view model. The quantitative results in Sec. 4.1 support this finding. The first two rows show that applying FLUX [24] to enhance the training A-pose images leads to an improvement in FID. Although LPIPS, PSNR, and SSIM are only marginally affected, this enhancement proves to be valuable, as demonstrated in the last two rows. When generating free-view images using a back-view synthesized by a model trained on an FLUX-enhanced dataset (indicated by a checkmark in the FLUX column), we observe consistent improvements across all evaluation metrics.

5. Discussion: End-to-End vs. Stage-by-Stage

The quantitative results of the End-to-End (E2E) pipeline and the Stage-by-Stage (SBS) pipeline are reported in

Tab. 3. Comparing the second and fourth rows, both models are trained solely on MVHumanNet, SBS demonstrates significant improvements in LPIPS, PSNR, and SSIM, though it is slightly less effective in FID. This suggests that SBS better preserves pairwise consistency, especially in image quality after pose transfer.

To further improve synthesis quality, we incorporate VTON data into training for both E2E and SBS pipelines. However, in the E2E pipeline, we observe a decline in performance after introducing VTON data (as shown in the first row). We hypothesize that this degradation is caused by imbalanced conditioning of E2E model with inconsistent data forms between the two datasets. In E2E, MVHumanNet provides controls over face, clothing, shoes, and various poses/views, whereas VTON mainly consists of frontal-view, close-up photographs that often depict only the upper body or lack facial information. When aligning VTON data to be jointly trained with MVHumanNet, the missing disentangled controls are set to \emptyset (e.g., a black image) to match classifier-free guidance training [15]. This misalignment in disentangled factors leads to the observed degradation.

By adopting the stage-by-stage pipeline, we ensure that only Stage 3 (free-view synthesis) is trained on the combined MVHumanNet and VTON datasets. Since VTON lacks front-back A-pose human images, the inputs for front-back view A-pose humans from VTON are set as \emptyset . Thus, VTON contributes only to pose-to-image training. Compared to E2E framework, which entangles multiple factors, Stage 3 in SBS focuses solely on pose and texture conditioning. This targeted optimization allows the SBS pipeline trained on MVHumanNet and VTON to achieve significant improvements. As shown in Fig. 7, SBS outperforms E2E, and the strategy trained with VTON dataset produces textures more consistent with the ground truth.

6. Conclusion

We introduce a new and challenging task in human image synthesis that controls viewpoint, pose, clothing, and identity within a unified framework. While an end-to-end model offers a straightforward approach, our analysis reveals its limitations in generalizability, particularly when trained on datasets with inconsistent conditioning factors. To address this, we propose a stage-by-stage framework, which significantly enhances pose and viewpoint control while improving robustness to in-the-wild scenarios. Our experiments demonstrate that structured factor disentanglement leads to improved synthesis quality, particularly in zero-shot settings. By leveraging dataset specialization in different stages, our method enables more effective utilization of available data, outperforming existing approaches in view and pose control. We hope our findings on end-to-end vs. stage-by-stage synthesis will inspire further research in controllable human generation.

References

- [1] Sizhe An, Hongyi Xu, Yichun Shi, Guoxian Song, Umit Y. Ogras, and Linjie Luo. Panohead: Geometry-aware 3d full-head synthesis in 360deg. In *CVPR*, 2023. 2
- [2] Qingyan Bai and Yujun Shen. Real-time 3d-aware portrait editing from a single image. *ArXiv*, 2024. 2
- [3] Ankan Kumar Bhunia, Salman Khan, Hisham Cholakkal, Rao Muhammad Anwer, Jorma Laaksonen, Mubarak Shah, and Fahad Shahbaz Khan. Person image synthesis via denoising diffusion model. In *Proceedings of the IEEE/CVF Conference on Computer Vision and Pattern Recognition*, pages 5968–5976, 2023. 3
- [4] Andrew Brock. Large scale gan training for high fidelity natural image synthesis. *arXiv preprint*, 2018. 2
- [5] Eric R. Chan, Connor Z. Lin, Matthew A. Chan, Koki Nagano, Boxiao Pan, Shalini De Mello, Orazio Gallo, Leonidas J. Guibas, Jonathan Tremblay, Sameh Khamis, Tero Karras, and Gordon Wetzstein. Efficient geometry-aware 3d generative adversarial networks. In *Proceedings of the IEEE/CVF Conference on Computer Vision and Pattern Recognition (CVPR)*, pages 16123–16133, 2022. 2
- [6] Seunghwan Choi, Sunghyun Park, Minsoo Lee, and Jaegul Choo. Viton-hd: High-resolution virtual try-on via misalignment-aware normalization. In *Proceedings of the IEEE/CVF Conference on Computer Vision and Pattern Recognition (CVPR)*, pages 14131–14140, 2021. 2, 4, 11
- [7] Yunjey Choi, Minje Choi, Munyoung Kim, Jung-Woo Ha, Sunghun Kim, and Jaegul Choo. Stargan: Unified generative adversarial networks for multi-domain image-to-image translation. In *Proceedings of the IEEE Conference on Computer Vision and Pattern Recognition (CVPR)*, 2018. 2
- [8] Yisol Choi, Sangkyung Kwak, Kyungmin Lee, Hyungwon Choi, and Jinwoo Shin. Improving diffusion models for authentic virtual try-on in the wild. In *Computer Vision – ECCV 2024*, pages 206–235, Cham, 2025. Springer Nature Switzerland. 2, 4, 6
- [9] Zijian Dong, Xu Chen, Jinlong Yang, Michael J Black, Otmar Hilliges, and Andreas Geiger. Ag3d: Learning to generate 3d avatars from 2d image collections. In *Proceedings of the IEEE/CVF international conference on computer vision*, pages 14916–14927, 2023. 3
- [10] Patrick Esser, Sumith Kulal, Andreas Blattmann, Rahim Entezari, Jonas Müller, Harry Saini, Yam Levi, Dominik Lorenz, Axel Sauer, Frederic Boesel, et al. Scaling rectified flow transformers for high-resolution image synthesis. In *Forty-first International Conference on Machine Learning*, 2024. 5, 6
- [11] Anna Frühstück, Krishna Kumar Singh, Eli Shechtman, Niloy J. Mitra, Peter Wonka, and Jingwan Lu. Insetgan for full-body image generation. In *Proceedings of the IEEE/CVF Conference on Computer Vision and Pattern Recognition (CVPR)*, pages 7723–7732, 2022. 2, 3
- [12] Jianglin Fu, Shikai Li, Yuming Jiang, Kwan-Yee Lin, Chen Qian, Chen Change Loy, Wayne Wu, and Ziwei Liu. Stylegan-human: A data-centric odyssey of human generation. In *Computer Vision – ECCV 2022*, pages 1–19, Cham, 2022. Springer Nature Switzerland. 2, 3
- [13] Ian Goodfellow, Jean Pouget-Abadie, Mehdi Mirza, Bing Xu, David Warde-Farley, Sherjil Ozair, Aaron Courville, and Yoshua Bengio. Generative adversarial nets. *Advances in neural information processing systems*, 27, 2014. 2
- [14] Xiao Han, Xiatian Zhu, Jiankang Deng, Yi-Zhe Song, and Tao Xiang. Controllable person image synthesis with pose-constrained latent diffusion. In *Proceedings of the IEEE/CVF International Conference on Computer Vision*, pages 22768–22777, 2023. 3
- [15] Jonathan Ho and Tim Salimans. Classifier-free diffusion guidance. *arXiv preprint arXiv:2207.12598*, 2022. 8
- [16] Fangzhou Hong, Zhaoxi Chen, Yushi Lan, Liang Pan, and Ziwei Liu. Eva3d: Compositional 3d human generation from 2d image collections. *arXiv preprint arXiv:2210.04888*, 2022. 2, 3
- [17] Fangzhou Hong, Zhaoxi Chen, Yushi LAN, Liang Pan, and Ziwei Liu. EVA3d: Compositional 3d human generation from 2d image collections. In *The Eleventh International Conference on Learning Representations*, 2023. 3
- [18] Li Hu. Animate anyone: Consistent and controllable image-to-video synthesis for character animation. In *Proceedings of the IEEE/CVF Conference on Computer Vision and Pattern Recognition*, pages 8153–8163, 2024. 3, 7
- [19] Tero Karras, Timo Aila, Samuli Laine, and Jaakko Lehtinen. Progressive growing of GANs for improved quality, stability, and variation. In *International Conference on Learning Representations*, 2018. 2
- [20] Tero Karras, Samuli Laine, and Timo Aila. A style-based generator architecture for generative adversarial networks. In *Proceedings of the IEEE/CVF Conference on Computer Vision and Pattern Recognition (CVPR)*, 2019. 2
- [21] Tero Karras, Samuli Laine, Miika Aittala, Janne Hellsten, Jaakko Lehtinen, and Timo Aila. Analyzing and improving the image quality of stylegan. In *Proceedings of the IEEE/CVF Conference on Computer Vision and Pattern Recognition (CVPR)*, 2020. 2
- [22] Rawal Khirodkar, Timur Bagautdinov, Julieta Martinez, Su Zhaoen, Austin James, Peter Selednik, Stuart Anderson, and Shunsuke Saito. Sapiens: Foundation for human vision models. In *European Conference on Computer Vision*, pages 206–228. Springer, 2025. 11
- [23] Alexander Kirillov, Eric Mintun, Nikhila Ravi, Hanzi Mao, Chloe Rolland, Laura Gustafson, Tete Xiao, Spencer Whitehead, Alexander C. Berg, Wan-Yen Lo, Piotr Dollar, and Ross Girshick. Segment anything. In *Proceedings of the IEEE/CVF International Conference on Computer Vision (ICCV)*, pages 4015–4026, 2023. 6
- [24] Black Forest Labs. Flux. <https://github.com/black-forest-labs/flux>, 2024. 6, 8
- [25] Sangyun Lee, Gyojung Gu, Sunghyun Park, Seunghwan Choi, and Jaegul Choo. High-resolution virtual try-on with misalignment and occlusion-handled conditions. In *European Conference on Computer Vision*, pages 204–219. Springer, 2022. 2, 4
- [26] Heyuan Li, Ce Chen, Tianhao Shi, Yuda Qiu, Sizhe An, Guanying Chen, and Xiaoguang Han. Spherehead: Stable 3d full-head synthesis with spherical tri-plane representation, 2024. 2

- [27] Connor Z. Lin, David B. Lindell, Eric Chan, and Gordon Wetzstein. 3d gan inversion for controllable portrait image animation. *ArXiv*, abs/2203.13441, 2022. 2
- [28] Xingchao Liu, Chengyue Gong, and Qiang Liu. Flow straight and fast: Learning to generate and transfer data with rectified flow. *arXiv preprint arXiv:2209.03003*, 2022. 5
- [29] Ziwei Liu, Ping Luo, Xiaogang Wang, and Xiaoou Tang. Deep learning face attributes in the wild. In *IEEE International Conference on Computer Vision*, 2015. 2
- [30] Yongyi Lu, Yu-Wing Tai, and Chi-Keung Tang. Attribute-guided face generation using conditional cycleGAN. In *Proceedings of the European Conference on Computer Vision (ECCV)*, 2018. 2
- [31] Yanzuo Lu, Manlin Zhang, Andy J Ma, Xiaohua Xie, and Jianhuang Lai. Coarse-to-fine latent diffusion for pose-guided person image synthesis. In *Proceedings of the IEEE/CVF Conference on Computer Vision and Pattern Recognition*, pages 6420–6429, 2024. 3, 7
- [32] Davide Morelli, Matteo Fincato, Marcella Cornia, Federico Landi, Fabio Cesari, and Rita Cucchiara. Dress code: High-resolution multi-category virtual try-on. In *Proceedings of the IEEE/CVF Conference on Computer Vision and Pattern Recognition (CVPR) Workshops*, 2022. 2, 4, 11
- [33] Georgios Pavlakos, Vasileios Choutas, Nima Ghorbani, Timo Bolkart, Ahmed A. A. Osman, Dimitrios Tzionas, and Michael J. Black. Expressive body capture: 3d hands, face, and body from a single image. In *Proceedings of the IEEE/CVF Conference on Computer Vision and Pattern Recognition (CVPR)*, pages 10975–10985, 2019. 2, 5
- [34] William Peebles and Saining Xie. Scalable diffusion models with transformers. In *Proceedings of the IEEE/CVF International Conference on Computer Vision (ICCV)*, 2023. 2
- [35] Kripasindhu Sarkar, Lingjie Liu, Vladislav Golyanik, and Christian Theobalt. Humangan: A generative model of human images. In *2021 International Conference on 3D Vision (3DV)*, pages 258–267, 2021. 2, 3
- [36] Ruizhi Shao, Youxin Pang, Zerong Zheng, Jingxiang Sun, and Yebin Liu. Human4dit: 360-degree human video generation with 4d diffusion transformer. *arXiv preprint arXiv:2405.17405*, 2024. 3
- [37] Fei Shen, Hu Ye, Jun Zhang, Cong Wang, Xiao Han, and Wei Yang. Advancing pose-guided image synthesis with progressive conditional diffusion models. *arXiv preprint arXiv:2310.06313*, 2023. 3
- [38] Jiaxin Xie, Hao Ouyang, Jingtan Piao, Chenyang Lei, and Qifeng Chen. High-fidelity 3d gan inversion by pseudo-multi-view optimization. In *Proceedings of the IEEE/CVF Conference on Computer Vision and Pattern Recognition*, pages 321–331, 2023. 2
- [39] Zhangyang Xiong, Di Kang, Derong Jin, Weikai Chen, Linchao Bao, Shuguang Cui, and Xiaoguang Han. Get3dhuman: Lifting stylegan-human into a 3d generative model using pixel-aligned reconstruction priors. In *Proceedings of the IEEE/CVF International Conference on Computer Vision*, pages 9287–9297, 2023. 3
- [40] Zhangyang Xiong, Chenghong Li, Kenkun Liu, Hongjie Liao, Jianqiao Hu, Junyi Zhu, Shuliang Ning, Lingteng Qiu, Chongjie Wang, Shijie Wang, Shuguang Cui, and Xiaoguang Han. Mvhumannet: A large-scale dataset of multi-view daily dressing human captures. In *Proceedings of the IEEE/CVF Conference on Computer Vision and Pattern Recognition (CVPR)*, pages 19801–19811, 2024. 2, 5, 7, 11
- [41] Yuhao Xu, Tao Gu, Weifeng Chen, and Chengcai Chen. Oot-diffusion: Outfitting fusion based latent diffusion for controllable virtual try-on. *arXiv preprint arXiv:2403.01779*, 2024. 4
- [42] Zhongcong Xu, Jianfeng Zhang, Jun Hao Liew, Hanshu Yan, Jia-Wei Liu, Chenxu Zhang, Jiashi Feng, and Mike Zheng Shou. Magicanimate: Temporally consistent human image animation using diffusion model. In *Proceedings of the IEEE/CVF Conference on Computer Vision and Pattern Recognition*, pages 1481–1490, 2024. 3, 7
- [43] Shuai Yang, Zhangyang Wang, Jiaying Liu, and Zongming Guo. Deep plastic surgery: Robust and controllable image editing with human-drawn sketches. In *ECCV*. Springer, 2020. 2
- [44] Hu Ye, Jun Zhang, Sibio Liu, Xiao Han, and Wei Yang. Ip-adapter: Text compatible image prompt adapter for text-to-image diffusion models. *arXiv preprint*, 2023. 6
- [45] Jianhao Zeng, Dan Song, Weizhi Nie, Hongshuo Tian, Tongtong Wang, and An-An Liu. Cat-dm: Controllable accelerated virtual try-on with diffusion model. In *Proceedings of the IEEE/CVF Conference on Computer Vision and Pattern Recognition (CVPR)*, pages 8372–8382, 2024. 2, 4
- [46] Chi Zhang, Yiwen Chen, Yijun Fu, Zhenglin Zhou, Gang Yu, Billzb Wang, Bin Fu, Tao Chen, Guosheng Lin, and Chunhua Shen. Styleavatar3d: Leveraging image-text diffusion models for high-fidelity 3d avatar generation. *arXiv preprint arXiv:2305.19012*, 2023. 3
- [47] Hongwen Zhang, Yating Tian, Yuxiang Zhang, Mengcheng Li, Liang An, Zhenan Sun, and Yebin Liu. Pymaf-x: Towards well-aligned full-body model regression from monocular images. *IEEE Transactions on Pattern Analysis and Machine Intelligence*, 45(10):12287–12303, 2023. 11
- [48] Lvmin Zhang, Anyi Rao, and Maneesh Agrawala. Adding conditional control to text-to-image diffusion models. In *Proceedings of the IEEE/CVF International Conference on Computer Vision (ICCV)*, pages 3836–3847, 2023. 6
- [49] Xuanmeng Zhang, Jianfeng Zhang, Rohan Chacko, Hongyi Xu, Guoxian Song, Yi Yang, and Jiashi Feng. Getavatar: Generative textured meshes for animatable human avatars. In *Proceedings of the IEEE/CVF International Conference on Computer Vision*, pages 2273–2282, 2023. 3
- [50] Zerong Zheng, Han Huang, Tao Yu, Hongwen Zhang, Yandong Guo, and Yebin Liu. Structured local radiance fields for human avatar modeling. In *Proceedings of the IEEE/CVF Conference on Computer Vision and Pattern Recognition*, pages 15893–15903, 2022. 6, 7, 11
- [51] Zerong Zheng, Xiaochen Zhao, Hongwen Zhang, Boning Liu, and Yebin Liu. Avatarrex: Real-time expressive full-body avatars. *ACM Transactions on Graphics (TOG)*, 42(4): 1–19, 2023. 6, 7, 11

Exploring Disentangled and Controllable Human Image Synthesis: From End-to-End to Stage-by-Stage

Supplementary Material

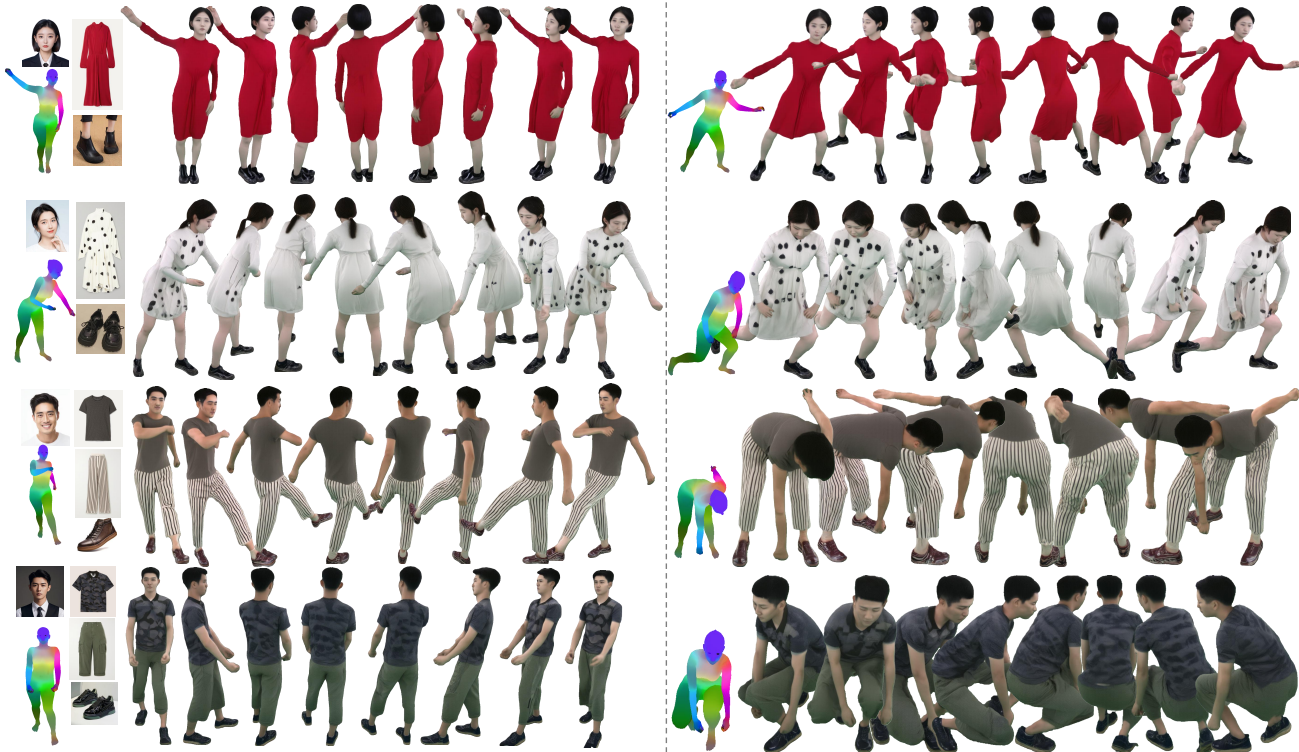


Figure 8. More results on the Stage-by-Stage (SBS) pipeline.

7. Datasets Preparation

MVHumanNet The MVHumanNet dataset [40] consists of multi-view videos of 9,000 subjects wearing various outfits. It provides annotations for human foreground masks, camera poses, and SMPLX estimations. Each subject includes a calibrated A-pose frame and is captured by multi-view cameras. To ensure data quality, we use only the 6,000 high-quality subjects, as some subjects have inconsistent camera settings. Images are extracted from video frames, and to reduce the dataset size, we select 8 evenly spaced frames per video and 4 specific camera views (front, left, back, right) for training, yielding a total of 192k training images. For testing, the dataset provides 400 test subjects, from which we select 2 frames per video and 4 camera views per subject, resulting in 3.2k test images.

For training the end-to-end pipeline, we extract face, upper clothing, lower clothing, dress, and shoes from each subject’s calibrated A-pose frame using the Sapiens segmentation model [22]. The A-pose frame is not included in the training set but is used to provide disentangled inputs. To support more customizable inputs, the end-to-end

pipeline is trained with images from both front and back views. For simplicity, these additional views are not depicted in Fig. 2 and Fig. 3.

VTON The term “VTON dataset” in this paper refers to a combination of two virtual try-on datasets: VITON-HD [6] and DressCode [32]. Both datasets provide human parsing annotations and flattened in-shop clothing images. We use PyMAF-X [47] for SMPLX estimations. The training set consists of 60k images. Since these datasets contain only limited viewpoints and poses, we do not use them for model evaluation.

THuman 4.0 THuman 4.0 [50] contains only three subjects. Due to its limited size, we use this dataset exclusively for zero-shot testing.

AvatarReX AvatarReX [51] provides multi-view videos of four subjects. We select around 900 frames in total from THuman4.0 and AvatarReX to construct a zero-shot test set.

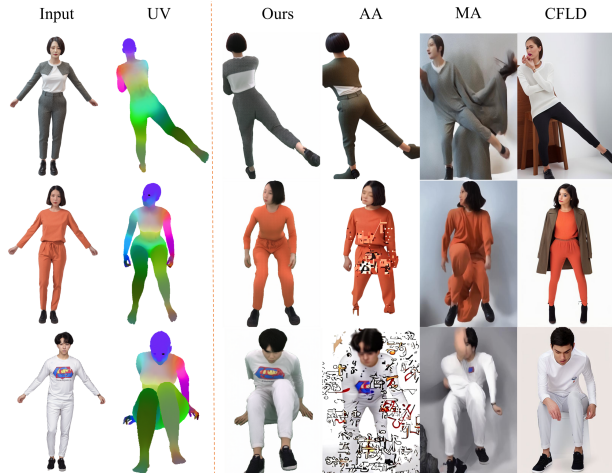


Figure 9. More qualitative zero-shot inference results of different methods on in-the-wild full-body human images generated by Stable Diffusion.

8. User Study on In-the-Wild Data

We conducted a user study to evaluate the effectiveness of our method on in-the-wild data. We randomly selected 30 cases, each containing four synthesized images generated by the four models under the same input conditions. A total of 50 participants were asked to vote for the image they perceived as the most realistic by considering: view consistency, pose accuracy, identity consistency, and texture fidelity. The results are shown in Tab. 4.

Ours	AnimateAnyone	MagicAnimate	CFLD
71.2%	21.8%	2.6%	4.4%

Table 4. User study results on in-the-wild data. The table shows the percentage of votes received by each method, where a higher percentage indicates stronger user preference.

9. Limitations and Future Work

One limitation of our approach lies in the diffusion model’s tendency to produce artifacts in smaller regions of the image, such as fingers and faces, due to their relatively small size compared to the entire picture. Consequently, the synthesized results from DiscoHuman occasionally exhibit imperfections in these areas. However, this limitation can be mitigated through post-processing methods that do not require additional fine-tuning. For example, utilizing the ADetailer plugin[†] effectively addresses these artifacts. This plugin re-generates the face and hand regions with a larger cropped resolution and seamlessly pastes the improved re-

[†]ADetailer plugin: <https://github.com/Bing-su/adetailer>

gions back into the original image, significantly enhancing the overall quality. Future work could explore integrating such post-processing techniques directly into the generation pipeline for a more streamlined and robust output.